Materials and Design 85 (2015) 687–694

Contents lists available at ScienceDirect

Materials and Design

journal homepage: www.elsevier.com/locate/jmad

Valorization of co-combustion fly ash in concrete production

Flora Faleschini [a], Mariano Angelo Zanini [a], Katya Brunelli [b], Carlo Pellegrino [a,*]

[a] Dept. of Civil, Environmental and Architectural Engineering, University of Padova, Via Marzolo 9, 35131 Padova, Italy
[b] Dept. of Industrial Engineering, University of Padova, Via Marzolo 9, 35131 Padova, Italy

ARTICLE INFO

Article history:
Received 10 April 2015
Received in revised form 26 June 2015
Accepted 14 July 2015
Available online 18 July 2015

Keywords:
Fly ash
Co-combustion
Mechanical strength
Durability
Wetting-drying cycles
Microstructure

ABSTRACT

The purpose of this paper is to compare the effects of two different Supplementary Cementing Materials (SCMs) on mechanical and durability-related properties of structural concrete. Three mixes were produced, where coal and co-combustion fly ashes were used as partial substitute of cement (20% in volume) and compared with a control/reference concrete. Performances investigated included fresh concrete properties, compressive and tensile strength, elastic modulus, permeability, capillarity and drying/wetting resistance. Results indicate that both the SCMs can be classified as low-carbon fly ashes, and their use in concrete improves the workability of the mixes. A slight reduction of mechanical strength was observed for the concretes including both the SCMs. In addition, concrete transport properties were also slightly reduced when co-combustion fly ash was used. Wetting-drying cycles affected significantly the durability of all the mixes: compressive strength after these cycles was significantly lowered, and the cracks occurred due to the thermal stress applied, appeared to be filled by needle-shape crystals of ettringite.

1. Introduction

The use of secondary fuels in coal-fired power plants plays an important role in reducing the emissions of carbon in the atmosphere due to energy industry. A number of experiments with different supplementary fuels are reported in literature, i.e., with municipal sewage sludge, biomass, and refuse-derived fuels [1–6]. Between these, refuse-derived fuels (RDFs), also known as solid recovered fuels (SRFs), are already applied in full-scale coal-fired power plants, such as at the "Andrea Palladio" plant at Fusina, owned by Ente Nazionale per l'Energia eLettrica (ENEL), the major Italian energy provider, and located close to the petrochemical facility of Porto Marghera within the Venice lagoon (Italy). In this plant two thermoelectric units are equipped with a RDF storage, dosage and feeding system; each line is designed for a maximum throughput of 9 t/h, corresponding to 70,000 t/year and about 5% of the whole thermal input. RDF is obtained from the separation of the high calorific fraction from municipal solid waste, through a mechanical–biological treatment, and it mainly consists in paper and plastics, with minor content of wood and textile. This material has a relatively high lower heating value (LHV) with respect to other supplementary fuels, which makes it particularly suitable for the intended application: it is characterized by an average LHV of 17 MJ/kg, greater than residual waste (10.617 MJ/kg) and paper sludge (2.537 MJ/kg) [3,7]. According to the production data of 2013, this plant produces about 49,000 t/y of coal-fly ash (CFA), and about 155,000 t/y of co-combustion fly ash (CCFA).

A fundamental issue that should be investigated when using supplementary fuels relates to the quality of fly ash produced during the combustion, as it may be a valuable resource in concrete industry. Coal fly ash has been successfully used in concrete industry since more than 50 years, primarily as mineral admixture in Portland cement concrete and also as a component of blended cement [8]. Concerning its first use, fly ash can either partially substitute Portland cement or be applied as an addition into ready-mix concrete at the batch plant [9,10]. It is generally accepted that the use of those Supplementary Cementing Materials (SCMs) promotes sustainability of concrete industry. Usual structural and durability-related properties were widely analyzed in literature [11–14]. In addition, several authors have attempted to relate some properties of SCM-concretes with parameters such as fly ash fineness [15], glass phase content [16] soluble and reactive silica content [17], water to powder ratio [18] and curing conditions [19]. Despite a wide literature concerning coal fly ash use as mineral admixture, up to now few works analyzed the application of fly ashes from co-combustion processes in concrete industry, and they are generally focused on a limited number of properties, i.e., cement setting time and compressive strength [20,21], concrete slump and mechanical strength [2].

According to the above concepts, the work shown in this paper aims to characterize the fly ash produced by the full scale power plant of Fusina (Italy), where coal is co-combusted with RDF, and analyzing some mechanical and durability-related properties of concretes, including fly ash as 20% of replacement of cement. Results are compared with a control/reference concrete without any mineral addition, and another concrete including coal-fly ash produced in a different thermoelectric unit of the same plant, where only coal is combusted.

* Corresponding author.
E-mail address: carlo.pellegrino@unipd.it (C. Pellegrino).

http://dx.doi.org/10.1016/j.matdes.2015.07.079
0264-1275/

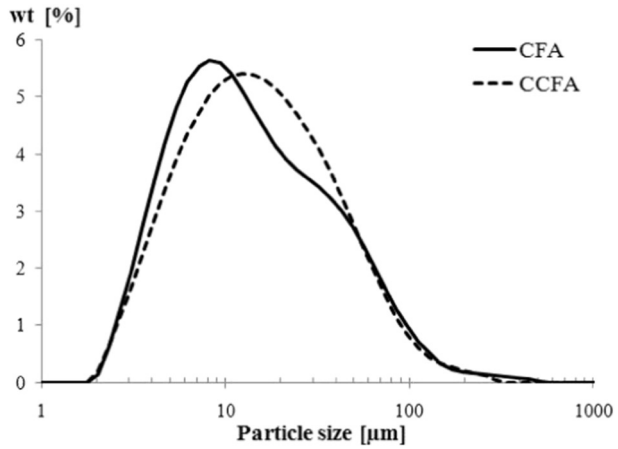

Fig. 1. Grain size distribution of CFA and CCFA.

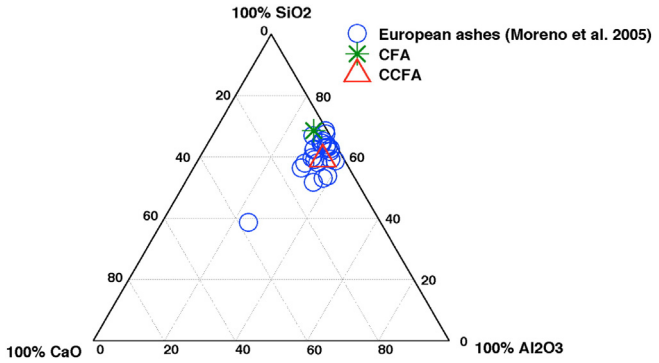

Fig. 2. Ternary diagram of the average bulk composition of CFA and CCFA.

2. Fly ashes' and cement characterization

Two types of fly ashes are used in this work: a light-brown coal-fly ash (CFA) and a dark-gray co-combustion fly ash (CCFA), both produced at the Fusina power plant (Italy). The ashes and the cement were subjected to a physical–chemical, mineralogical and morphological characterization.

The particle size distributions of both the FAs and cement were determined by means of laser diffraction particle size analyses. Fig. 1 shows the grain size distribution of the considered FAs. CFA has a two-modal distribution, and it is characterized by the following percentile values of the distribution: $d_{10} = 4.305$ μm; $d_{50} = 12.481$ μm; $d_{90} = 55.506$ μm. CCFA has a Gaussian monomodal distribution, with: $d_{10} = 4.589$ μm; $d_{50} = 14.494$ μm; $d_{90} = 52.43$ μm. Cement has a two-modal distribution, characterized by $d_{10} = 1.35$ μm, $d_{50} = 10.68$ μm and $d_{90} = 32.75$ μm, being finer than the FAs used in this work. Both the FAs have very small dimension, with about 35% of particles with less than 10 μm dimension (PM_{10}): low particles size, high fineness, and consequently high surface area are generally advantageous for the pozzolanic reactivity of the material [22], and also for the packing effect and filling the voids in the cement matrix. The specific surface areas are 3100 cm^2/kg and 2860 cm^2/kg respectively for CFA and CCFA, and 4790 cm^2/kg for the cement. In this case, the FAs' specific surface area and particles size are in the same order of magnitude of cement. The true density was obtained with the pycnometer method, where kerosene was used as fluid, and it results in the range of 2035–2140 kg/m^3 for both the FAs, and of 3080 kg/m^3 for the cement.

Chemical composition was obtained by means of X-ray fluorescence spectrometry (XRF), using an Automated XRF Thermo Scientific ARL Advant'X, and major compounds of FAs and cement are listed in Table 1. Accordingly, both FAs can be classified as low-calcium fly ashes [23].

Loss on ignition (LOI) of solid combustion residues was determined according to [24]: this value indicates that CCFA has a relatively high unburned carbon content. During the test, due to coal burning, CCFA changed color from dark gray to brown. Water content and LOI values are also reported in Table 1, as well as pH and conductivity values, obtained from suspensions prepared mixing 10 g of FAs powder (or cement), and 100 mL of de-ionized water, after 10 min of stirring. The values are in agreement with other results obtained in literature, using the same liquid/solid (L/S) ratio in aqueous suspension [25]. CCFA has a slightly higher conductivity than CFA due to the presence of a greater amount of unburned carbon, which is more conductive than the non-conducting alumino-silicate glassy microsphere particles occupying the largest volume of the fly ash mixture [26].

Fly ashes bulk composition is represented in Fig. 2, within the data of other ashes reported in Moreno et al. [27].

X-ray diffraction (XRD) technique was used to qualitatively identify the crystalline phases of the FAs. A Siemens D500 diffractometer, with a stepped and continuous scanning device, with nickel-filtered CuKα ($\lambda = 1.5405$ Å), at 40 kV and 30 mA, was used. Results are represented in Fig. 3: the major non-reactive phases in both the FAs are hematite (Fe_2O_3), mullite ($Al_6Si_2O_{13}$) and quartz (SiO_2). Those phases usually characterize low-calcium ashes [28]. In addition, peaks corresponding to magnetite (Fe_3O_4) and kyanite (Al_2SiO_5) were found in CFA, whereas sillimanite (Al_2SiO_5) is present in CCFA. The glass content, which is visible in the XRD patterns as a background, is about the 70 wt.% for CFA according to the semi-quantitative estimation of mineral phases made in Moreno et al. [27].

Scanning electron microscope (SEM) images were taken both in the secondary-electrons (SE) mode, with an acceleration voltage of 15 kV, and in the backscattered electrons (BSE) mode, using an accelerating voltage of 25 kV. A stereoscan equipped with an energy dispersive X-

Table 1
Major chemical compounds of FAs and cement (SD = standard deviation).

Compound	CFA [%]	SD [%]	CCFA[%]	SD [%]	OPC [%]	SD [%]
Na_2O	2.04	±0.19	1.18	±0.17	2.00	±0.22
MgO	1.971	±0.06	1.693	±0.054	2.583	±0.074
Al_2O_3	21.36	±0.07	28.48	±0.08	5.77	±0.036
SiO_2	52.77	±0.10	48.48	±0.09	21.61	±0.05
SO_3	1.158	±0.006	0.5598	±0.0036	4.114	±0.013
K_2O	1.872	±0.013	0.8597	±0.0094	0.9796	±0.0055
CaO	2.978	±0.014	4.863	±0.017	61.39	±0.09
Fe_2O_3	7.690	±0.015	3.422	±0.009	2.670	±0.006
LOI	3.63	–	6.50	–	2.10	–
Water content	0.8	–	0.4	–	0.1	–
pH	10.5	–	11	–	12	–
Conductivity [μS/cm]	1351	–	1682	–	10,880	–

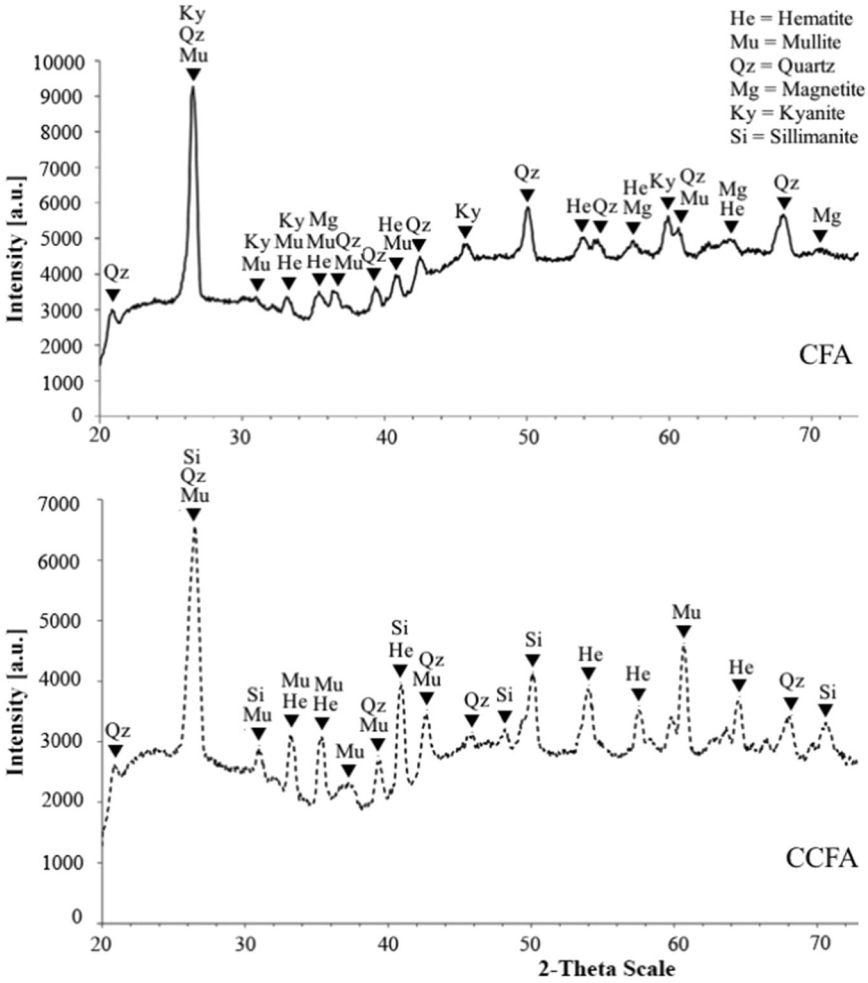

Fig. 3. Comparison of XRD patterns of CFA (upper) and CCFA (lower).

ray spectroscopy (EDS) system was used, and samples were sputtered with gold before the analyses. Figs. 4–5 show images of CFA and CCFA, taken at a magnification of 1000×: based on EDS results, samples appear as composed of small spherical particles, with medium-size conglomerate particles formed by alumino-silicate matter, and medium-to-small compact heavy metal-rich particles (mostly Fe), which appears brighter. The texture of both the FAs appears smooth, despite the relative high LOI value, indicating that they underwent an incomplete burning. A pleroshere filled by microsphere is also shown in a CCFA sample.

3. Experimental investigation on SCM-concrete

3.1. Materials

The materials used for all the mixes are: ordinary Portland cement type I 52.5R class, as defined in EN 197-1 [29] and experimentally analyzed above; natural sand with a 6.3 mm maximum size as fine aggregate; natural coarse aggregates with a 22.4 mm maximum size; a super-plasticizing sulphonated naphtalene admixture; tap water; CFA and CCFA described in the previous section.

3.2. Mix details

Three different concrete mixtures were produced: the first was used as control, and it does not contain any mineral admixture. The others contained CFA and CCFA respectively, with a cement replacement ratio equal to 20% by volume. This value has been chosen accordingly to the objective of achieving environmental gains in terms of reduced emissions, without affecting significantly concretes' properties. Additionally, the replacement ratio satisfies the EN 206 provisions, being the fly ash/cement ratio equal to 0.2 in mass, below the limit of 0.33 for CEM I type [30]. Water-to-binder ratio, Bolomey aggregates grading curve, super plasticizing admixture content were kept almost constant for all the batches. Table 2 illustrates the details of the mix proportions, chosen to reach the following concrete performances: water-to-binder ratio less or equal to 0.5, S4 consistency class according to EN 206-1 [29], cylindrical/cubic compressive strength after 28 days greater than 30/35 MPa. During the production of CCFA mix, the water content was slightly reduced because of the high workability reached by the fresh concrete.

3.3. Experimental methods

After mixing, specimens were properly compacted, covered to limit evaporation, demolded 24 h after casting, and then cured in standard temperature (20 ± 2 °C) and humidity (RH ≥ 95%) conditions until the time of testing.

Compressive strength was measured after 7, 28 and 90 days on cubic specimens with 150 mm side [31] with a universal testing machine Galdabini, type Sun/60, with a load capacity of 600 kN. Cylindrical specimens with 100 mm diameter and 200 mm length were used for measuring tensile strength by means of splitting test [32]. Secant modulus of elasticity was evaluated according to [33].

Durability-related properties were analyzed using the following tests performed after a 28 days standard maturation: water absorption test under atmospheric condition [34], water depth penetration under

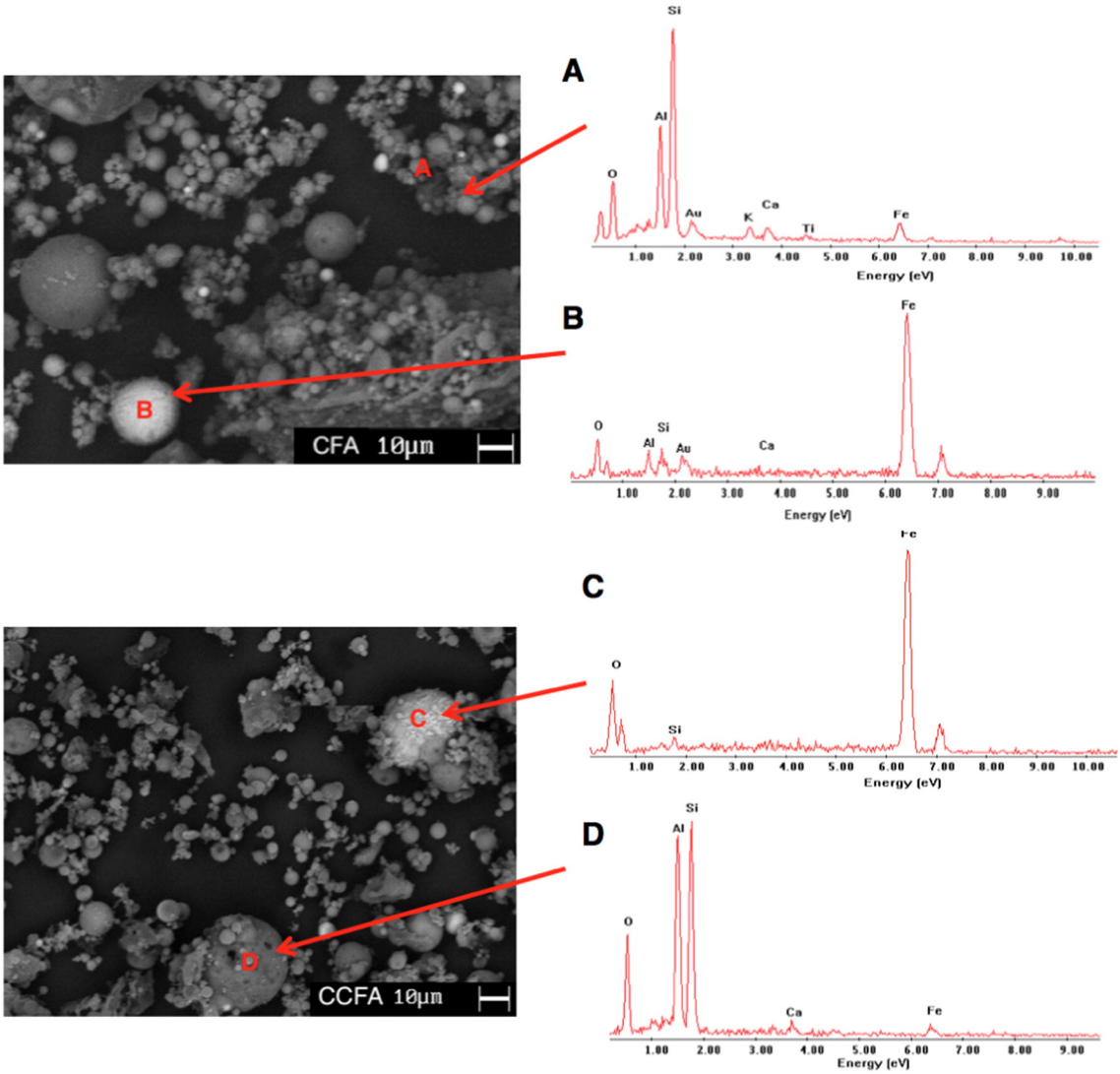

Fig. 4. BSE–SEM images of CFA (upper left) and CCFA (upper right).

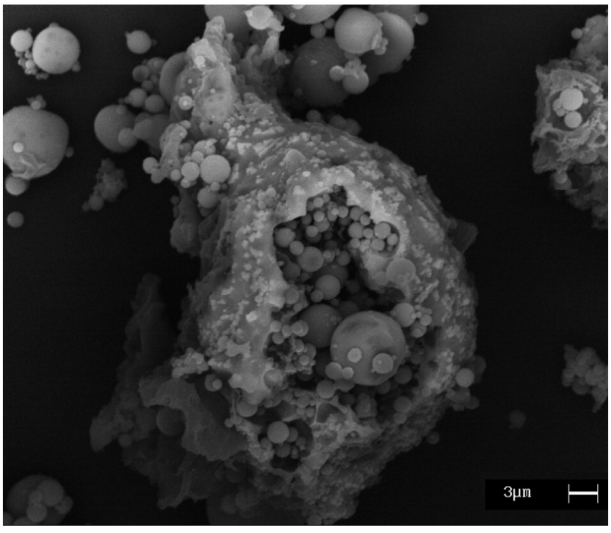

Fig. 5. BSE–SEM image of a pleroshere in a CCFA sample.

pressure [35], and compressive strength tests after wetting/drying cycles. Water absorption was evaluated on 100 mm (diameter) x 200 mm (height) cylindrical specimens, preliminary dried at 110 °C in an electric oven for 24 h. Then they were dipped in water, with a 5 mm emerging side in the first 24 h; subsequently, they were completely submerged for other 6 days. Specimens weight is measured after 1, 3, 8, 24 h, 3, 7 days and then water absorbed is expressed as its percentage on the dried weight. Water depth penetration is measured on 100 × 100 mm

Table 2
Mix design.

	Control mix	CFA mix	CCFA mix
Cement [kg/m^3]	300	240	240
CFA [kg/m^3]	–	48	–
CCFA [kg/m^3]	–	–	48
W / (C + FA)	0.5	0.5	0.47
Water [kg/m^3]	150	144	136
Coarse aggregates [kg/m^3]	1030	1030	1030
Fine aggregates [kg/m^3]	1030	1030	1030
SP [kg/m^3]	3	3	3

Table 3
Fresh concrete properties and mechanical strength at 28 days.

	Control mix	CFA mix	CCFA mix
Fresh concrete properties			
Density [kg/m^3]	2438	2380	2438
Slump [mm]	180	200	200
Mechanical strength — 28 days			
Density [kg/m^3]	2436	2428	2434
$f_{cm,cube}$ [MPa]	40.7	38.97	39.80
f_{ctm} [MPa]	3.66	3.59	3.94
E_{cm} [GPa]	31.96	30.64	30.20

cylindrical specimens subjected to a water pressure of 500 ± 50 kPa for 72 h. Then the specimens were cut, and the water profile was measured on the splitting surfaces. Detrimental cycles were performed on 100 × 200 mm cylindrical specimens: the test consisted in 30 daily cycles, in which the specimens were completely immersed in potable water at room temperature for 16 h, and then dried at 110 ° C in electric oven for the remaining 8 h.

For each test, at least three specimens were used and the mean value of these is reported.

4. Results and discussion

4.1. Mechanical strength and fresh concrete properties

The concretes produced in this experimental campaign belong to the S4 consistency class, with a slump value equal to s = 19 ± 1 cm. Fresh concrete properties are listed in Table 3 together with the results of mechanical strength tests, including compressive, tensile strength and elastic modulus. The use of FA improves the workability of both the SCM-concretes, due to the small round-shape and smooth texture of the particles observed by SEM images, which could be advantageous from the water demand point of view [22]. Regarding compressive strength, its evolution in time is plotted in Fig. 6. As expected, when SCM partially replaces cement, strength slightly reduces if compared with that of the traditional mix, mainly due to the lower cement content rather than for slower hydration and pozzolanic reactions, occurring for low calcium fly ashes [36]. The strength loss is generally similar at each concrete age: the reduction of the gap between control/traditional and FA concrete in time, often reported in literature, is not observed in this work. This can be due to their lower content in available active silica with respect to most of the FAs used in literature, and also to the relatively high water content used in this work. The efficacy of using FAs as partial cement replacement is highly influenced by W / (C + FA)

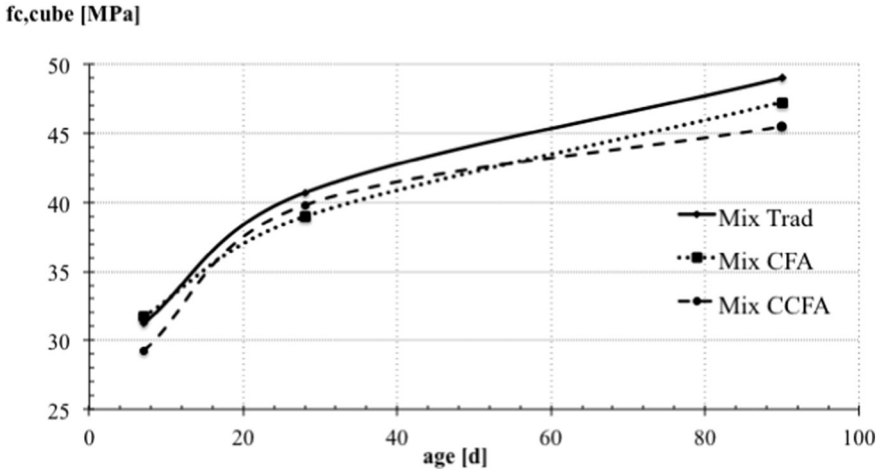

Fig. 6. Compressive strength evolution vs. concrete age.

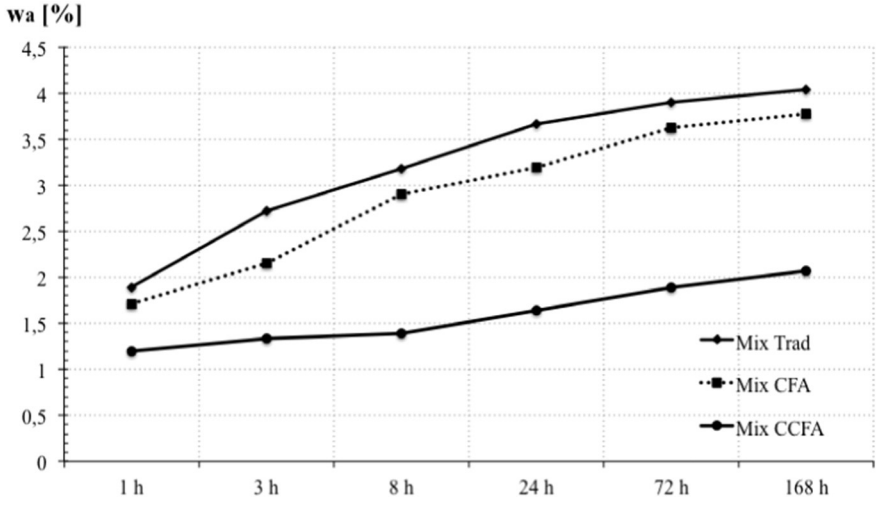

Fig. 7. Water absorption vs. time.

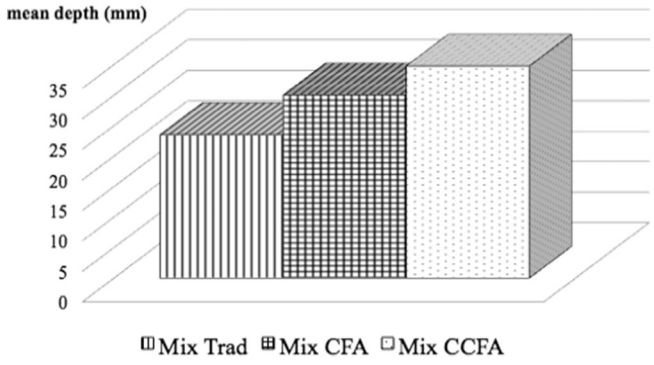

Fig. 8. Mean water penetration depth.

ratio: it is demonstrated that strength reductions are recovered only when low water-to-binder ratios are used [37]. In addition, tensile strength is improved of 7.65% when CCFA is used as partial cement replacement. Elastic modulus is slightly reduced in SCM-concretes, with a maximum loss of 5.5% for the CCFA mix.

4.2. Concrete transport properties

Water absorption at atmospheric pressure is defined as the increase in mass of the specimens, expressed as a percentage of the oven-dried mass, due to the quantity of the water absorbed per unit of concrete volume. It can be expressed as:

$$W_i = (M_i - M_0)/M_0 \cdot 100 \quad (1)$$

where W_i is the absorption at time i, M_i is the mass at time i, and M_0 is the mass oven-dried of the specimen. The cumulative water absorption in time is plotted in Fig. 7: the effect of the FAs is beneficial in both the SCM concretes, resulting in a decrease of the water absorbed, most significant with the increase of time in the case of CCFA substitution.

Water penetration depth was measured on specimens subjected to a hydraulic pressure equal to 500 kPa: results indicate that the partial substitution of the traditional binder slightly increases the water depth profile, for both the analyzed fly ashes, as shown in Fig. 8. This result is in line with the slight reduction in compressive strength. According to the results of water absorption and water penetration tests it is possible to state that SCM-concretes have a lower porosity matrix, i.e., the volume of pore space in these concretes seems less than in the control/reference mix. Conversely, as the permeability is a measure of the open porosity, it is possible to assume that the pores seem more connected in the SCM-concretes. Additionally, the slight worse behavior of concretes with FAs against water penetration is in agreement with the results of compressive strength test (see Fig. 6), being both affected by the quality of the cementitious matrix. However, a proper verification of this result should be confirmed by an analysis of the specimens' microstructure.

Table 4
Strength loss due to wetting/drying cycles.

	Control mix	CFA mix	CCFA mix
Mechanical strength — 28 days			
Density [kg/m^3]	2436	2428	2434
$f_{cm,cube}$ [MPa]	40.7	38.97	39.80
Mechanical strength — W/D cycles			
Density [kg/m^3]	2452	2434	2530
$f_{cm,cube}$ [MPa]	32.20	30.72	28.38
$\Delta f_{cm,cube}$ [%]	−20.88	−21.17	−28.69

4.3. Resistance against wetting/drying cycles

Alternate wetting/drying cycles are very detrimental for concrete: they accelerate the damage due to salts crystallization in the pores of the conglomerates, and determine deterioration due to thermal stress. The main effect is the decrease of concrete mechanical strength, i.e., the loss of compressive strength, which occurred for each mix tested. In addition, a gain of weight of the dry-surface specimens was observed for each concrete, which was more significant for the CCFA mix. This could be caused to the cracks' opening, through which water can enter into the specimen. Results after the 30 daily cycles applied to the analyzed specimens are reported in Table 4.

Concrete surfaces exposed to environmental cycles were analyzed by means of SEM test to check the potential of delayed ettringite formation (DEF), and analyze the paste-aggregates bond surface after the compressive strength test. The extent of damage observed during this work leads to the assumption that another damaging action could be involved, such as the one caused by massive ettringite formation. Often DEF (also known as secondary ettringite) has been found in concretes exposed to heat treatment at high temperature, generally above 70 °C [38,39]. Its formation has been associated to several causes, including pre-damage of concrete, sulfates and alkali content. In general it is possible to state that DEF occurs in concretes with particular compositional characteristics (SO_3 content in cement around 4% or more), that have undergone heating until 70 °C or more, and which have been exposed to a moisture environment [40]. In this case, the source of sulfates, which determines an internal attack as defined by Collepardi [41], can be imputed to the relatively high SO_3 content of the cement used in this work, which is about 4.11% of cement weight (see Table 1). According to Batic et al. [42] wetting/drying cycles cause large expansion and concrete cracking, and this phenomenon can be attributed mainly to two causes. On one side, there is the action of the water inside the pores and the cracks, especially in the smallest ones, due to the orientation of water dipoles, which determine significant pressure inside concrete matrix. On the other side, massive ettringite formation participates in concrete damage, even if it is not already clear if it represents the cause or the effect of the expansion. It should be noted that the presence of ettringite does not mean that a damage has occurred, and the simple presence of ettringite in cracks is not diagnostic of DEF-related damage [43].

Concerning the influence of fly ash, it generally decreases the expansion due to DEF, and this is partially due to the increased Al_2O_3 content in the binder, available for sulfoaluminate formation [44].

On those bases, SEM images were taken in the SE mode with an acceleration voltage of 15 kV, on samples obtained after compressive strength test, which were sputtered with gold. Energy Dispersive X-ray spectroscopy (EDS) system was used for the microanalysis. The traditional concrete, when not subjected to any detrimental treatment,

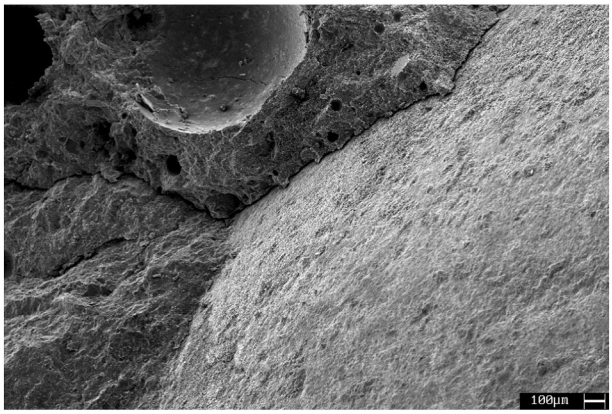

Fig. 9. SE–SEM magnified view of a crack between aggregate and cement paste (control mix).

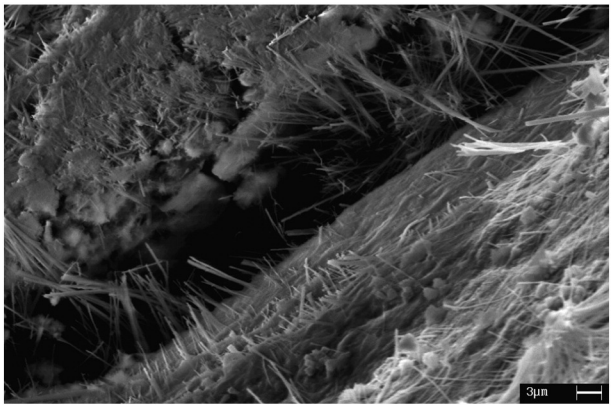

Fig. 10. SE–SEM image of needle-shape crystals filling a micro-crack (CFA mix).

was not damaged and it appeared rather dense (Fig. 9): cracks mainly occurred between the cement paste and the aggregate, and developed through the less resistant part of the matrix, i.e., air voids.

When the specimens were subjected to wetting/drying cycles, the matrix appeared, from a visual inspection, more brittle than the case without cycles. This occurred for all the mixes: SEM images show micro-cracks with a width of 2–5 μm on the surface of the binder matrix (Fig. 10), which is directly related to the strength reduction shown in Table 4. Cracks appeared to be filled by needle-shape crystals, which were also abundant on concrete surface. Based on EDS analysis, those needles can be identified as ettringite (Fig. 11): the presence of traces of gold is just due to the specimen preparation procedure. Strength reduction can be also associated to the heterogeneous expansion due to secondary ettringite formation in the hardened concrete, which is mainly located in the cracks or in the existing weakness produced by the thermal stress applied with the treatment. The use of fly ash did not exhibit any additional benefits in wetting/drying resistance, probably due to the high water-to-binder ratio used in this work, which results in a high rate of water transport in the matrix.

5. Conclusions

The use of RDF in the Fusina thermal plant allows saving of about 5% of non-renewable resources, contributing to reduce the environmental impacts of the energy industry. When supplementary fuels are used, the quality of the ashes should be analyzed to use them in building materials, because they can be a valuable resource.

According to the results obtained in this work, the following conclusions can be drawn with reference to this specific CCFA:

- The CCFA has a higher content of unburned carbon than CFA, due to the co-combustion process where RDF and coal are burned together. Additionally, it has a lower fineness and specific surface than CFA, resulting in a slightly lower quality fly ash;
- The fineness, the small round shape and the smooth texture of FAs improve concrete workability;
- The use of the SCMs in partial replacement of cement results in a slight decrease in compressive strength of concretes. This gap is not reduced with the curing age, as expected, because of the high W / (C + FA) content used in this experimental campaign. Nevertheless, this reduction does not exceed the 5% in all the analyzed cases, and the produced concretes satisfy the minimum requirements defined in Section 3.2;
- The use of CCFA slightly decreases transport properties of the concrete: on one side, the overall porosity of the matrix is reduced, but on the other side the pores appear to be more connected and, as a consequence, its permeability is higher;
- Wetting/drying cycles are very detrimental for the tested concrete: the compressive strength, measured after the treatment, was 20% lower than without any cycles for all the mixes (including control/reference mix). The extent of the damage lead to state that, within the micro-cracking due to the high thermal stress, massive ettringite formation could be involved. Micro-cracks were found to be filled by needle-shape ettringite crystals. The effect of the SCMs was not relevant against wetting/drying resistance.

This work gives some elements for encouraging the use of potentially huge quantities of CCFA for concrete engineering applications and can pave the ground for a more complete assessment of the potential application of various types of fly ashes from co-combustion processes in concrete industry. A particular attention should be paid to fly ash fineness, texture, unburned carbon and glassy phase content, within bulk oxides composition, which are parameters affecting fresh and hardened concrete properties. In addition, their elemental composition should be analyzed to check the environmental compatibility.

Acknowledgments

The authors would like to acknowledge Eng. Fausto Bassi from the Andrea Palladio thermoelectric plant (owned by ENEL S.p.A.), Mr. Daniele Pozzobon from Cementi Candeo S.p.A. respectively for supplying the fly ashes and the cement. The authors acknowledge also Mr. Paolo Maria Vendramini and Mr. Alejandro Vázquez Capitas for their help during the experimental campaign.

References

[1] N. Wolski, J. Maier, K.R.G. Hein, Fine particle formation from co-combustion of sewage sludge and bituminous coal, Fuel Process. Technol. 85 (6–7) (2004) 673–686.
[2] A.J. Sarabèr, Co-combustion and its impact on fly ash quality; full-scale experiments, Fuel Process. Technol. 128 (2014) 68–82.
[3] H. Wu, A.J. Pedersen, P. Glarborg, F.J. Frandsen, K. Dam-Johansen, B. Sander, Formation of fine particles in co-combustion of coal and solid recovered fuel in a pulverized coal-fired power station, Proc. Combust. Inst. 33 (2011) 2845–2852.

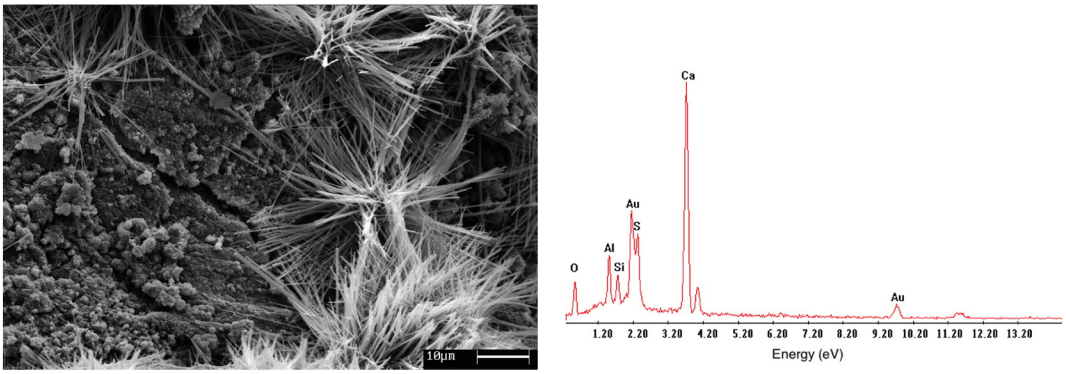

Fig. 11. On the left: needle-shape crystals. On the right: EDS spectrum.

[4] L. Rigamonti, M. Grosso, L. Biganzoli, Environmental assessment of refuse-derived fuel co-combustion in a coal-fired power plant, J. Ind. Ecol. 16 (5) (2012) 748–760.
[5] A. Islam, U.J. Alengaram, M.Z. Jumaat, I.I. Bashar, The development of compressive strength of ground granulated blast furnace slag-palm oil fuel ash-fly ash based geopolymer mortar, Mater. Des. 56 (2014) 883-841.
[6] T. Sinsiri, W. Kroehong, C. Jaturapitakkul, P. Chindaprasirt, Assessing the effect of biomass ashes with different finenesses on the compressive strength of blended cement paste, Mater. Des. 42 (2012) 424–433.
[7] H.-P. Wan, Y.-H. Chang, W.-C. Chien, H.-T. Lee, C.C. Huang, Emissions during co-firing of RDF-5 with bituminous coal, paper sludge and waste tires in a commercial circulating fluidized bed co-generation boiler, Fuel 87 (6) (2008) 761–767.
[8] N. Bouzoubaâ, M.-H. Zhang, V.M. Malhotra, D.M. Golden, Blended fly ash cements — a review, ACI Mater. J. 96 (6) (1999) 641–650.
[9] R. Siddique, J.M. Khatib, Abrasion resistance and mechanical properties of high-volume fly ash concrete, Mater. Struct. 42 (5) (2010) 709–718.
[10] R. Siddique, Properties of self-compacting concrete containing class F fly ash, Mater. Des. 32 (3) (2011) 1501–1507.
[11] V.G. Papadakis, S. Tsimas, Supplementary cementing materials in concrete. Part I: efficiency and design, Cem. Concr. Res. 32 (2002) 1525–1532.
[12] V.G. Papadakis, S. Antiohos, S. Tsimas, Supplementary cementing materials in concrete. Part II: a fundamental estimation of the efficiency factor, Cem. Concr. Res. 32 (2002) 1533–1538.
[13] D.F. Aponte, M. Barra, E. Vàzquez, Durability and cementing efficiency of fly ash in concrete, Constr. Build. Mater. 30 (2012) 537–546.
[14] M. Arezoumandi, J.S. Volz, C.A. Ortega, J.J. Myers, Effect of total cementitious content on shear strength of high-volume fly ash concrete beams, Mater. Des. 46 (2013) 301–309.
[15] D.P. Bentz, E.J. Garboczi, Simulation studies of the effects of mineral admixtures on the cement paste–aggregate interfacial zone, ACI Mater. J. 88 (5) (1991) 518–529.
[16] K.L. Aughenbaugh, R.T. Chancey, P. Stutzman, M.C. Juenger, D.W. Fowler, An examination of the reactivity of fly ash in cementitious pore solutions, Mater. Struct. 46 (2013) 869–880.
[17] R.V. Ranganath, B. Bhattacharjee, S. Krishnamoorthy, Influence of size fraction of ponded ash on its pozzolanic activity, Cem. Concr. Res. 28 (5) (1998) 749–761.
[18] R. Siddique, P. Aggarwal, Y. Aggarwal, Influence of water/powder ratio on strength properties of self-compacting concrete containing coal fly ash and bottom ash, Constr. Build. Mater. 29 (2012) 73–81.
[19] A.F. Bingöl, I. Tohumcu, Effects of different curing regimes on the compressive strength properties of self compacting concrete incorporating fly ash and silica fume, Mater. Des. 51 (2013) 12–18.
[20] A.J. Sarabèr, Co-combustion and its impact on fly ash quality; pilot-scale experiments, Fuel Process. Technol. 104 (2012) 105–114.
[21] E. Tkaczewska, R. Mróz, G. Łój, Coal–biomass fly ashes for cement production of CEM II/A-V 42.5R, Constr. Build. Mater. 28 (2012) 633–639.
[22] P. Chindaprasirt, S. Homwuttiwong, V. Sirivivatnanon, Influence of fly ash fineness on strength, drying shrinkage and sulfate resistance of blended cement mortar, Cem. Concr. Res. 34 (2004) 1087–1092.
[23] ASTM C618-12a, Standard specification for coal fly ash and raw or calcined natural pozzolan for use in concrete, American Society for Testing and Materials, Annual Book of ASTM Standards, vol. 04.02, 2012 (West Conshohocken, PA).
[24] EN 196–2, Method of Testing Cement — Part 2: Chemical Analysis of Cement, Comité Européen de Normalisation, Brussels, Belgium, 2013.
[25] J. Payá, J. Monzó, M.V. Borrachero, E. Peris-Mora, Mechanical treatment of fly ashes. Part I: physico-chemical characterization of ground fly ashes, Cem. Concr. Res. 25 (1995) 1469–1479.
[26] H. Choo, N.N.N. Yeboah, S.E. Burns, Impact of unburned carbon particles on the electrical conductivity of fly ash slurry, J. Geotech. Geoenviron. Eng. ASCE 140 (04014052) (2014) 1–9.
[27] N. Moreno, X. Querol, J.M. Andrés, K. Stanton, M. Towler, H. Nugteren, M. Janssen-Jurkovicová, R. Jones, Physico-chemical characteristics of European pulverized coal combustion fly ashes, Fuel 84 (2005) 1351–1363.
[28] R. Dhole, M.D.A. Thomas, K.J. Folliard, T. Drimalas, Characterization of fly ashes for sulfate resistance, ACI Mater. J. 110 (2) (2013) 159–168.
[29] EN 197-1, Cement — Part 1: Composition, Specification and Conformity Criteria for Common Cements, Comité Européen de Normalisation, Brussels, Belgium, 2006.
[30] EN 206, Concrete: Specification, Performance, Production and Conformity, Comité Européen de Normalisation, Brussels, Belgium, 2013.
[31] EN 12390-4, Testing Hardened Concrete – Compressive Strength – Specification for Testing Machines, Comité Européen de Normalisation, Brussels, Belgium, 2000.
[32] EN 12390-6, Testing Hardened Concrete — Tensile Splitting Strength of Test Specimens, Comité Européen de Normalisation, Brussels, Belgium, 2009.
[33] EN 12390-13, Testing Hardened Concrete — Determination of Secant Modulus of Elasticity in Compression, Comité Européen de Normalisation, Brussels, Belgium, 2013.
[34] UNI 7699, Testing Hardened Concrete — Determination of Water Absorption at Atmospheric Pressure, Ente Nazionale Italiano di Unificazione, Milano, Italia, 2005. (in Italian).
[35] EN 12390-8, Testing Hardened Concrete — Depth of Penetration of Water Under Pressure, Comité Européen de Normalisation, Brussels, Belgium, 2009.
[36] V.G. Papadakis, Effect of fly ash on Portland cement systems: part I. Low-calcium fly ash, Cem. Concr. Res. 29 (1999) 1727–1736.
[37] M.R.H. Dunstan, Fly ash as the 'fourth ingredient' in concrete mixtures, ACI SP 91 (1986) 171–200.
[38] S. Diamond, Delayed ettringite formation — process and problems, Cem. Concr. Compos. 18 (1996) 205–215.
[39] I. Odler, Y. Chen, On the delayed expansion of heat cured portland cement pastes and concrete, Cem. Concr. Compos. 18 (1996) 181–185.
[40] A. Pavoine, X. Brunetaud, L. Divet, The impact of cement parameters on delayed ettringite formation, Cem. Concr. Compos. 34 (2012) 521–528.
[41] M. Collepardi, A state-of-the-art review on delayed ettringite attack on concrete, Cem. Concr. Compos. 25 (2003) 401–407.
[42] O. Batic, C.A. Milanesi, P.J. Maiza, S.A. Marfil, Secondary ettringite formation in concrete subjected to different curing conditions, Cem. Concr. Res. 30 (9) (2000) 1407–1412.
[43] K. Scrivener, J.P. Skalny, Conclusions of the International RILEM TC 186-ISA Workshop on Internal Sulfate Attack and Delayed Ettringite Formation (4–6 September 2002, Villars, Switzerland), Mater. Struct. 38 (2005) 659–663.
[44] H.F.W. Taylor, C. Famy, K.L. Scrivener, Delayed ettringite formation, Cem. Concr. Res. 31 (2001) 683–693.